Tree-ring reconstruction of snow avalanche activity: Does avalanche path selection matter?

G. de Bouchard d'Aubeterre, A. Favillier, R. Mainieri, J. Lopez Saez, Nicolas Eckert, M. Saulnier, J. Peiry, M. Stoffel, Christophe Corona

Tree-ring reconstruction of snow avalanche activity: Does avalanche path selection matter?

de Bouchard d'Aubeterre G. [1], Favillier A. [1,*], Mainieri R. [2], Lopez Saez J. [3], Eckert N. [5], Saulnier M. [6], Peiry, J-L. [7], Stoffel M. [3,4,8], Corona C. [1]

1. Université Clermont Auvergne, CNRS, Université de Limoges, GEOLAB, F-63000 Clermont-Ferrand, France.

2. University Grenoble Alpes, Irstea, UR LESSEM, 2 rue de la Papeterie-BP 76, F-38402 St-Martin-d'Hères, France.

3. Institute for Environmental Sciences – University of Geneva, 66 Boulevard Carl Vogt, CH-1205 Genève, Switzerland.

4. Dendrolab.ch, Department of Earth Sciences, University of Geneva, rue des Maraîchers 13, CH-1205 Geneva, Switzerland.

5. Univ. Grenoble Alpes, IRSTEA, UR ETNA, 38402 St-Martin-d'Hères cedex France.

6. Faculty of Forestry and Wood Sciences, Czech University of Life Sciences, Kamýcká 129, 16521 Prague, Czech Republic.

7. CNRS, UMI3189, « Environnement, Santé, Sociétés », Faculté de Médecine, UCAD, BP 5005, DAKAR-FANN, Sénégal.

8. Department F.-A. Forel for Environmental and Aquatic Sciences, University of Geneva, 66 Boulevard Carl-Vogt, CH-1205 Geneva, Switzerland.

* Corresponding author: GEOLAB UMR 6042 – Maison des Sciences de l'Homme, 4 rue Ledru 63057 Clermont-Ferrand CEDEX 1, France.

E-mail address: adrien.favillier@uca.fr

Abstract

In the current context of anthropogenic global warming, one of the purposes of dendrogeomorphic analyses is to provide long and continuous chronologies of mass movements, so as to detect potential trends or shift related to increasing temperatures. However, on documented slopes, the comparison between historical archives and tree-ring records suggests that dendrogeomorphic reconstructions systematically underestimate the natural activity of the process under investigation. In the specific case of snow avalanches, underestimation generally amounts to 50% and the main causes generally given for this difference are related to the magnitude of past events. In this study, we hypothesize that the morphometric characteristics of avalanche paths and their forest cover could have significant impacts on the length and reliability of tree-ring reconstructions. In order to test this hypothesis, we selected four adjacent, albeit differently structured, avalanche paths from the Queyras massif (French Alps), with the aim to compare their potential for a continuous reconstruction of past avalanche activity. On the most active avalanche paths characterized by high-altitude release areas (covered only by shrubby vegetation), tree-ring reconstructions do not exceed one century in length, with recurrence intervals of high magnitude events > 25 years. By contrast, on forested couloirs where lower slopes and forest coverage up to the release areas limits the intensity of events, the frequency of reconstructed snow avalanches is 2.5 times higher, the reconstructions span

longer periods and the convergence rate with historical archives attest to the reliability of the dendrogeomorphic approach. These results suggest that a careful selection of couloirs is essential and that priority should be given to forested sites as (i) they allow for exhaustive and (ii) reliable reconstructions over (iii) long periods of time.

Keywords: dendrogeomorphology, snow avalanche, forest cover, reliable reconstruction, French Alps, tree-rings.

1. Introduction

Avalanches are one of the major natural hazards in mountain regions. Every year, they damage urban infrastructures, transportation networks and endanger human lives (Bründl et al., 2004). During the 2017-2018 winter season, 64 avalanche-related accidents were recorded in France, including 26 fatal accidents (ANENA, 2018). In recent decades, the expansion of urbanization in mountainous massifs, increasing mobility, and the diversification of winter recreation have led to an increase in avalanche risk (Einhorn et al., 2015; Nöthiger and Elsasser, 2004; Techel et al., 2016). In France, observations of avalanche events are documented in the *Enquête Permanente sur les Avalanches* (EPA; or permanent avalanche survey), a database that contains ~100,000 avalanche events for ~4000 recognized paths in the French Alps and the Pyrenees since the beginning of the 20th century (Bourova et al., 2016; Mougin, 1922). Data on avalanches are gathered by forest rangers, who also record various quantitative (e.g., runout altitudes, deposit volumes) and qualitative (e.g., flow regime, snow quality) data (Jamard et al., 2002). Despite its uniqueness, the quality of EPA records locally depends to a large extent on the rangers' careful data recording, a fact that makes certain local series of limited use (Eckert et al., 2007; 2010a). In addition, Teich et al. (2012) stated that in forested terrain, avalanches are sometimes poorly documented as they are not of key importance compared to large destructive events threatening settlements, infrastructure, and human lives in open terrain.

On wooded avalanche paths, forest stands act as protective barriers, or snow bridges in release areas (Bebi et al., 2009). Based on dendrogeomorphic approaches (Alestalo, 1971; Stoffel and Corona, 2014), focused on the identification and dating of growth disturbances in ring width series, trees can also be used to reconstruct past avalanche activity with annual resolution and for periods covering past decades to centuries (Butler and Sawyer, 2008) and to fill certain gaps in incomplete historical chronicles (Stoffel et al., 2010). Since the pioneer works in dendrogeomorphology (Burrows and Burrows, 1976; Butler, 1979; Carrara, 1979; Mears, 1975; Potter, 1969; Shroder, 1980, 1978), an increasing number of studies has focused on snow avalanches by using tree-ring analysis to reconstruct years of avalanche activity (Boucher et al., 2003; Casteller et al., 2007; Corona et al., 2013, 2012, 2010; Favillier et al., 2018, 2017; Garavaglia and Pelfini, 2011; Laxton and Smith, 2009; Muntán et al., 2004; Stoffel et al., 2006), to calibrate avalanche flow models (Casteller et al., 2008; Schläppy et al., 2014), to analyze the impact of ecological and anthropogenic disturbances on snow avalanche regimes (Germain et al.,

2005) or to identify the synoptic situations responsible for the triggering of regional snow avalanche activity (Casteller et al., 2011; Dubé et al., 2004; Germain et al., 2009; Muntán et al., 2009). In the current context of global warming (Gobiet et al., 2014), tree-ring reconstructions are also expected to provide insights into longer-term (multi-centennial) fluctuations of avalanche activity (Ballesteros-Cánovas et al., 2018; Corona et al., 2013; Heffernan, 2018; Schläppy et al., 2016; Stoffel and Corona, 2018).

However, on documented paths, comparison between observations listed in the EPA and tree-ring records suggests that the dendrogeomorphic reconstructions systematically underestimate years with natural avalanche activity (Corona et al., 2013, 2012, 2010; Schläppy et al., 2014). The main causes that are typically given for this difference are related to the magnitude of past events. Avalanches have to be of sufficient magnitude to create impacts on trees (Bartelt and Stöckli, 2001; Bebi et al., 2009). Conversely, major avalanches may remove or blur the evidence of previous or subsequent events in case large parts of the forest are destroyed (Bryant et al., 1989; Carrara, 1979), or disturb tree growth in such a way that younger events cannot be identified in the tree-ring record (Kogelnig-Mayer et al., 2011). In that regard, the morphometric characteristics of the avalanche path– through their influence on the frequency and/or magnitude of events and the long-term viability of the forest stand – are susceptible to have a significant impact on the completeness of the ensuing tree-ring reconstruction. We therefore hypothesize that, in the absence of anthropogenic interventions, the potential for a complete and continuous avalanche reconstruction could vary strongly amongst adjacent paths.

In order to test this hypothesis, (1) a dendrogeomorphic approach has been deployed on a slope of the upper Guil valley (Ristolas municipality, French Alps) in the Queyras massif. This slope was selected as it is composed of four avalanche paths characterized by comparably low anthropogenic interventions (i.e. very limited grazing or forest harvesting in the past) but marked differences in terms of morphology (starting zone altitudes and path lengths), avalanche dynamics (frequency and magnitude of events), and forest cover (i.e. forested paths and corridors characterized by a marked transverse zonation), thus enabling the comparison between reconstructions. In order to enhance the detection of snow avalanche years and to disentangle the potential effects of snow avalanches from disturbance pulses caused by climatic or exogenous factors, such as cold/dry years or larch budmoth outbreaks, the four-step procedure developed by Favillier et al. (2017) has been used. (2) The multi-centennial reconstructions are validated through comparison with historical chronicles, old maps, and aerial photographs. (3) Their comparison enables discussion of the dendrogeomorphic potential of each of the analyzed paths. This subsequently provides criteria that can, in the future, help to select the best sites for as complete as possible and continuous avalanche reconstructions, that are crucial for the detection of potential trends in avalanche activity related to climatic and other environmental changes.

2. Study site

The site under investigation is located on the western slope of the Upper Guil Valley, upstream from the Echalp hamlet, at the locality Ravin de la Salce (44°44'47" N, 6°59'42 E; Fig. 1). The talus slope covers an area of 1.47 km^2 and extends from the Guil thalweg (1740 m asl) to the Crête des Baysses (2700 m asl). The mean slopes in the upper part of the talus range between 35 and 40°, while the distal segment appears geometrically concave with mean slope angles comprised between 20 and 25°. The site is dominated by the Crête des Baysses, a 400-m schisto-calcareous rockwall cut by several subvertical faults oriented S-N and SW-NE (Lemoine and Tricart, 1986).

Climate is characterized by a mixed montane-Mediterranean to continental character (Touflan et al., 2010). According to to the data from the nearby meteorological station of Saint-Véran (2125 m asl), located 12 km south-west from the slope, annual temperature is -1.5 °C for the period 1981–2010 and average annual precipitation amounts to 710 mm. During winter, mean air temperature (DJF) is -5.3 °C while precipitation amounts to 127 mm. Precipitation falls primarily as snow from November to April. Average annual snowfall reached 320 cm (±183 cm) for the period 1928–2007. The forest cover is dominated by European larch (*Larix decidua* Mill.) between 1750 m and 2300 m asl. The understorey is dominated by herbaceous species and shrubs, namely *Rhododendron ferrugineum* L. (rhododendron), *Juniperus comunis* (common juniper) and *Vaccinium myrtillus* L. (bilberry).

3. Material and methods

3.1. Archival data on past events

First, we compiled a historical database of past snow avalanches at Ravin de la Salce using the EPA covering the period 1930-2013. Then, with the aim to complement the archival database, topographic maps and 19 aerial flight campaigns available from the French National Geographic Institute (IGN, at a scale of ca. 1:25,000) were used to detect evidence of damaging avalanche events since 1945.

3.2. Delineation of avalanche paths

The delineation of the avalanche paths at Ravin de la Salce is complex due to (i) multiple release areas and avalanche tracks in the eastern part of the slope, (ii) the absence of preferential flow paths, and (iii) the dense forest cover, which is effectively masking geomorphic evidence of past avalanche events in the western part of the study site. To precisely delineate the spatial extent of each path, we used the CLPA avalanche map (*Carte de Localisation des Phénomènes Avalancheux*) that complements the EPA and localizes the maximum lateral extent and runout elevations of avalanche paths as retrieved from historical testimonies and the analysis of aerial photographs (Bonnefoy et al., 2010). In addition, the numerical avalanche dynamics model RAMMS (Rapid Mass Movement System; Christen et al., 2010; Gruber and Bartelt, 2007; Rudolf-Miklau et al., 2015) – has been employed to estimate the spatial pattern of high magnitude avalanche events. RAMMS predicts avalanche runout

distances, flow velocities and impact pressures on three-dimensional digital terrain models based on a Voellmy-fluid friction model.

RAMMS simulations were based on a 5-m Digital Elevation Model (DEM) extracted from the IGN RGE ALTI® database. Slopes with angles ranging from 30 and 45° were considered as potential release areas (Salm, 1982; Schweizer, 2003). In order to refine the detection, these thresholds were adjusted to account for the potential bias induced by the DEM resolution (ARPA and CEMAGREF, 2008) according to the following formula:

$$\alpha_r = \alpha \times RES^{-0.075} \quad (1)$$

Where α_r is the corrected angle value, α is the angle value (30-45) and RES is the resolution of the DEM (here RES=5 m).

For each delineated release area, one single simulation was performed with the objective of delineating the area exposed to extreme avalanche events. To this aim, typical friction parameter values were used following the recommendations of Gruber and Bartelt (2007). Snow depth in the release areas were set to 2 m, which, according to Gaume et al. (2013), corresponds to a return period of more than 100 years in terms of three-day snowfall events at the site.

3.3. Sampling strategy, identification, dating, and classification of growth disturbances

To reconstruct past avalanche activity based on dendrogeomorphic techniques, trees were sampled along three longitudinal transects. The upper transect (T1, 2200-m asl) is located in the release area of the two westernmost paths delineated according to the procedure detailed above, and at timberline for the easternmost paths. The intermediate transect (T2, 2000-2100 m asl) is located in the median part of each path. Finally, T3 (1880-1950-m asl) is situated in the distal and concave segment of the couloirs.

In summer 2017, 342 increment cores (52, 127, 77, 86 on E1, E2, C1, and C2, respectively) from 306 European larch (*Larix decidua* Mill.) trees were collected using a Pressler increment borer. The position of each tree was recorded with a 1-m precision GPS device and measurements were taken for the tree (diameter at breast height) and the disturbed feature (type, height). In this study, several kinds of growth disturbances (GD) to trees most commonly attributed to snow avalanches such as abrupt growth suppressions (Butler and Malanson, 1985; Corona et al., 2012; Kogelnig-Mayer et al., 2013; Stoffel et al., 2013), impact scars (Corona et al., 2014; Stoffel and Perret, 2006; Trappmann et al., 2013), callus tissue (CT; Schneuwly et al., 2009b; Stoffel et al., 2010), tangential rows of traumatic resin ducts (TRD; Bollschweiler et al., 2008b; Schneuwly et al., 2009a; Stoffel and Hitz, 2008) as well as the initiation of compression wood (Butler et al., 2010; Timell, 1986) were retained in the analysis.

Following recent recommendations by Stoffel and Corona (2014), Tichavský and Šilhán (2016) and Šilhán and Stoffel (2015), old and young trees were considered in our sampling procedure in order to ensure the completeness of avalanche chronologies.

Sampling positions were optimized based on recommendations given by Stoffel et al. (2013). Sample preparation and analysis followed the procedures described in Stoffel and Bollschweiler (2008) and Stoffel et al. (2013). GD were visually identified in the tree-ring series and cross-dated against the Echalp (1338-2010) and Souliers (1448-2009) local reference chronologies computed from undisturbed trees (Corona et al., 2013; Saulnier et al., 2017). In a subsequent step, intensities were assigned to GDs in order to emphasize features that are clearly associated with avalanche activity and to discriminate these from disturbances possibly induced by other factors (Corona et al., 2012; Stoffel et al., 2013). GDs were classified based on the visual quality of the evidence of reactions within each sample according to the intensity scale presented in Kogelnig-Mayer et al. (2011): weak (intensity class 1), medium (intensity class 2), and strong (intensity class 3) reactions and clear evidence of injuries (intensity class 4) were thus distinguished.

The age structure of the stand was approximated by counting the number of tree rings of sampled trees. However, since the innermost rings of some trees were rotten and trees were not sampled at their stem base, the age structure might be strongly underestimated (Bollschweiler et al., 2008a). Nonetheless, as *L. decidua* has been shown repeatedly to recolonize surfaces cleared by snow avalanches or other mass-movement processes and established dominance within a few decades, we believe that our age distribution could help the documentation of destructive events at our study site (Stoffel et al., 2006; Van der Burght et al., 2012). As a consequence, in order to detect potential forest recolonization dynamics, individual tree ages were spatially interpolated using an inverse distance weighted interpolation algorithm using ArcGIS (IDW; ESRI, 2013; Kennedy, 2013).

3.4. Detection of past avalanche events in growth disturbance series

To detect past snow avalanche years – during which at least one snow avalanche is reconstructed in the selected paths – in the GD series, we adopted the four-step procedure (Fig. 2) developed by Favillier et al. (2017) (Please refer to it for more details). This approach addresses the necessity to disentangle the potential effects of snow avalanches from disturbance pulses caused by climatic or exogenous factors, such as cold/dry years or larch budmoth outbreaks. Based on this procedure, the minimum population threshold was set to 15 trees alive the t year. GD and index I (Shroder, 1978, Eq. 2) – used to discriminate potential avalanche and non-avalanche events – were defined according to the sample size following the recommendations of Butler and Sawyer (2008) and Corona et al. (2012).

$$I_t = ((\sum_{i=1}^{n} R_t)/(\sum_{i=1}^{n} A_t)) * 100 \quad (2)$$

where ΣR is the number of trees responding to an event in year *t*, and ΣA represents the number of trees alive in year *t* at the path scale, where the extension of each individual path is delineated according to Sect 3.1. In other words, the detection of avalanche events is made in each path independently, and with a definition of each path corresponding to avalanche flow physics.

In addition to the procedure described in Favillier et al. (2017), lowered thresholds were adopted to maximize the number of detected events without including exogenous noise. Additional events were only added if they exceeded the I threshold and if the number of GD was less than 1 under the GD threshold. According to the second step of the procedure (Fig. 2), climatic and ecological signals interfering with the dendrogeomorphic signal were identified. In total, 17 larch budmoth (LBM, *Zeiraphera diniana* Gn.; cf. Baltensweiler et al., 1977, and Kress et al., 2009) outbreak years (see Table 1) have been reconstructed and 34 characteristic narrow rings have been identified in the Southern/Intermediate French Alps since 1720 CE according to Saulnier et al. (2017). Similarly, 20 years with negative May-September anomalies of temperature and precipitation (with values exceeding 1.5 SD below the average) have been considered as extreme dry/cold years (Table 1) during the period 1720–2003 and according to the gridded HISTALP point temperature information (Efthymiadis et al., 2006) closest to the study site. Potential avalanche events detected in step 1 coinciding with LBM outbreak episodes or extremely cold/dry years were examined in more detail to avoid misclassification. According to the procedure, we systematically excluded growth suppressions from the account of GDs. Avalanche and non-avalanche years were discriminated at the path scale based on a threshold of 3 GDs (Fig. 2).

In the third step, levels of confidence – very high (vHLC, Wit > 0.3), high (HLC, 0.3 > Wit > 0.2) and medium (MLC, Wit < 0.2) –were distinguished for each detected event based on a weighted index factor (Wit, Eq. 3) accounting for the type and intensity of GDs (Favillier et al., 2017).

$$W_{it} = \frac{[(\sum_{i=1}^{n} T_i*7)+(\sum_{i=1}^{n} T_s*5)+(\sum_{i=1}^{n} T_m*3)+(\sum_{i=1}^{n} T_w*1)]}{\sum_{i=1}^{n} A_t} \quad (3)$$

where, for each year *t*,, T_i is the sum of trees with injuries; T_s is the sum of trees with strong GDs; T_m is the sum of trees with medium-intensity GDs; T_w represents the sum of trees with weak-intensity GDs, and where *A* gives the total number of trees alive in year *t*. Despite the precautions taken at each previous step, each additional event detected during step 1 and events coinciding with an ecological or a climatic year at step 2 were only rated with a low level of confidence (LLC) (Fig. 2).

In the last step, avalanche events and corresponding GDs were mapped using the ArcGis 10.2.1 Time Slider (ESRI, 2013; Kennedy, 2013). On the basis of the sampling transects, avalanche reaching the upper, intermediate, and lower transects were rated as eXtra-Large (XL), Large (L), Medium, (M) or Small (S), respectively. At the path scale, the annual probability for an avalanche event was computed by dividing the number of reconstructed events by the period covered by the reconstruction.

4. Results

4.1. Delineation of avalanche paths at Ravin de la Salce

At Ravin de la Salce, precise geomorphic mapping including field observations, interpretation of aerial photographs (CLPA), extent of past avalanche events derived from the EPA and flow extensions simulated with

228 the RAMMS numerical snow avalanche simulations revealed a minimum of four distinct avalanche paths, namely
229 (from west to east): E1 (19.7 ha, 1075 m long, 240 m wide, release area 2110-2180 m asl), E2 (25.3 ha, 1130 m
230 long, 255 m wide, 2140-2340 m asl), C1 (42 ha, 1515m long, 300 m wide, 2290-2520 m asl), and C2 (55 ha, 1725
231 m long, 366 m wide, 2430-2620 m asl) (Fig. 1b, 3; see Table 2). According to the performed RAMMS simulations,
232 the maximum velocities and pressures are significantly lower on E1/E2 (<10 $m.s^{-1}$ and 100 kPa) than on C1/C2
233 (>30$m.s^{-1}$, >300 kPa). E1 and E2 are covered by a dense larch forest from the top of the slope to the runout
234 zones. A characteristic transverse vegetation pattern can be observed across C1 and C2: the inner zone is
235 colonized by herbaceous and shrubby (*R. ferrugineum*, *J. communis*) formations, whereas *L. decidua* is dominant
236 in the outer zone.

237 *4.2. Snow avalanches recorded in historical archives*

238 Archival data on past events at Ravin de la Salce go back to 1930. The EPA inventoried 10 events on avalanche
239 paths E1 and E2, namely in 1930, 1947, 1951, 1959, 1961, 1973, 1977, 1986, 2003, and 2009. According to the
240 EPA database in which E1 and E2 paths were grouped in a unique couloir, the longest events would have
241 occurred on 25 February 1947, 24 February 1951, and 1959 (undated), reaching an altitude of < 1550 m asl.
242 Damage to the forest stands are reported for the snow avalanches that occurred in 1977 (undated) and on 16
243 December 2008. For the period 1930-2008, the mean recurrence intervals between two consecutive events is 8
244 years based on EPA records. The absence of avalanche events between 1930 and 1947 is probably due to the
245 absence of systematic observations during the interwar period and World War II. Similarly, due to the absence of
246 elements at risk, avalanche paths C1 and C2 do not contain any records of past events in the EPA. However, one
247 event was retrieved from the CLPA datasheet, pointing to an avalanche that would have occurred on 16
248 December 2008 in at least one of these couloirs. In addition, according to the diachronic comparison of aerial
249 photographs, evidence for at least two snow avalanche events can be found indirectly as they apparently
250 destroyed parts of forested stands C1-C2 between 1957–1962 and 2003–2009.

251 *4.3. Age structure of the stands*

252 Visual cross-dating of tree-ring samples was carried out by means of the skeleton plot method and primarily
253 based on the narrow rings of 1500, 1643, 1668, 1741, and 1906. After cross-dating, data on pith ages at breast
254 height indicate that the 306 trees sampled on the Ravin de la Salce slope are on average 171 years old (± 102
255 years). The oldest tree selected for analysis attained sampling height in 1398 (618 rings in 2016) while the
256 youngest tree reached breast height in 2010. Figure 4 shows that trees older than 300 years are mainly located
257 along the upper transect (T1) where the average age of individuals is 206 years (± 114 years). On T3, the mean
258 age of sampled trees is lower, especially for E1 and C1 paths (126 ± 81 years). The number of trees (n=15)
259 considered as a minimum for analysis in our 4-step procedure was exceeded in 1779 at E1, 1720 at E2, 1813 at

C1 and 1791 at C2. The sample size shows a clear increase in the 1860-70s at E1, E2, and C1, and in the 1920s at C2. A second step or increase is observed in the 1980s at E1 (Fig. 5).

4.4. Distribution of growth disturbances and chronology of avalanche events

Sampled cores allowed identification of 1591 GD in the tree-ring series for the period 1720–2016, of which 314 (19.4%) were considered strong avalanche indicators (Classes 3 or 4). Table 3 summarizes the types of GD as well as their intensity. TRDs and CW were the GDs most frequently (76.6%) identified in the samples, followed by growth suppressions (GS; 20%). By contrast, only 51 injuries were sampled, which represents 3.2 % of the dated disturbances. In total, 60.6% of the GDs were rated as weak, 20.0% as median and 16.2% as strong. The oldest GD identified in the tree-ring series was dated to 1496 CE, the most recent to 2016. Nearly every year exhibited GD in a small number of trees for the period 1780-2016 at E1 and E2. GDs were scarcer before1920 at C1 and C2.

The event-response histograms depicted in Fig. 5 summarize all reactions recorded in the trees along the four avalanche paths. In total, 22 (1779-2016), 23 (1720-2016), 2 (1812-2016), and 5 (1894-2016) avalanche events were reconstructed at sites E1, E2, C1, and C2, respectively. The highest percentages of disturbances were recorded in 1909 with It of 41.94 and 31.1 and a Wit of 1.39 and 0.78 at paths E1 and E2, respectively. In 2009, growth disturbances reached It values of 13.33 (Wit: 0.31), 23.88 (Wit: 0.93), and 26.03 (Wit: 1) at paths E1, C1, and C2, respectively. Finally, a large proportion of disturbances were dated to 1961 at paths E1, E2, and C1 (It: 17.65, 26.09, 17.54%; Wit: 0.47, 0.66, 0.53).

Based on potential interferences between the avalanche and exogenous signals in the dendrochronological series (step 2), and on the basis of the Weighted Index Factor (Wit; step 3, Fig. 6) that includes simultaneously for the type and intensities of growth disturbances, 16 and 10 events occurring during 19 different years were assigned with very high and high levels of confidence, respectively. By comparison, 24 events (22 years) characterized by a majority of weak and medium GDs, were reconstructed with a medium and low level of confidence. Amongst the 20 potential events that coincide with LBM outbreak episodes or extreme climatic years, 9 were excluded from the reconstruction and 11 were rated with a low level of confidence. With respect to the 1791-2014 and 1809-1998 periods – delimited by the first and the last observed events – and at the level of the slope scale, the mean recurrence intervals of snow avalanches are 10 and 9 years at E1 and E2, respectively. They exceed 20 years (24 years, 1961-2009; and 23 years, 1894-2009) at C1 and C2. The decades 1931-1940 (7 events) and 1971-1980 (6 events) are characterized by the highest avalanche activity; conversely, no event was reconstructed for the periods 1829-1853 and 1937-1956. In total, nine events occurred synchronously at E1 and E2, namely in 1909, 1934, 1936, 1961, 1973, 1979, 1998, 2004, and 2011 (Fig. 7).

4.4. Spatial extent of reconstructed events

Sampling along transects only allows a partial reconstruction of the spatial extent of past avalanche events and an estimation of the minimum longitudinal extent of past events. In total, 15 events reached the distal segment of the talus, 24 were reconstructed at the median transect level and 13 were limited to the upper part of the avalanche paths. All the events retrieved at C1 and C2 reached the lowest transect. Conversely, at E1 and E2, 37 out of 45 (82%) snow avalanches were limited to the upper (35.1%) or the median (64.9%) transects.

Figure 8 shows two high-magnitude events reconstructed from the dendrogeomorphic approach in 1962 and 2009. Based on the EPA inventory, we could reasonably attribute the 30 and 10 GDs observed at E2 and C1, respectively, to the event reported on 7 February 1961. This hypothesis is further supported by the diachronic analysis of the aerial photographs of 1956 and 1962 showing that a large part of the stands was destroyed at C1 and that larch trees were removed from the main track and in the lowest portion of E2, Fig. 8). In the same way, the snow avalanche documented on 17 December 2008 was retrieved through tree-ring analyses at C1 (16 GDs) and C2 (19 GDs) and could be precisely delineated based on the aerial photographs from 2005 and 2010.

Before 1945, aerial photographs are not available for our study site. The topographic maps of 1896 and 1930 did not provide insights into possible changes in the spatial extent of the forest stand. As a consequence, the events reconstructed with a high level of confidence in 1897, 1920, 1928, and 1930 could not be confirmed through diachronic analysis.

5. Discussion

5.1. Accuracy of the reconstructions

The study we report here employs dendrogeomorphic techniques on four adjacent, albeit differently structured, avalanche paths from the Queyras massif (French Alps), with the aim to compare their potential for a continuous reconstructions of past avalanche activity. In the global warming context, such reconstructions have proven to be particularly important to complement incomplete historical record and for the detection of potential climate-related trends in avalanche activity (Ballesteros-Cánovas et al., 2018). To reach this goal, we used the 4-step procedure developed by Favillier et al. (2017) (i) to disentangle snow avalanche signals in tree-ring series from signals induced by other external disturbances and (ii) to estimate the robustness of our tree-ring based snow avalanche reconstruction depending on the total number of disturbances (GD) and the percentage of trees impacted. Based on this procedure, 52 snow avalanche events were reconstructed in 38 different avalanche years. The reconstruction therefore complemented the historical chronology significantly with 10 new snow avalanche winters between 1930 and 2008, and by extending the series back to 1791 CE at E1. In total, 70% of the avalanche years listed in the EPA were retrieved, especially on paths E1 and/or E2 with the dendrogeomorphic approach, namely in 1930 (E1, C2), 1959 (E2), 1961 (E1, E2, C2), 1973 (E1, E2), 1977 (E1), 2003 (E1), and 2009 (E1, C1, C2).

Amongst these avalanche years, five could be reconstructed with very high levels of confidence. In particular, the extreme avalanche cycle of 16 December 2008, when 10 snow avalanches were reported in the Ristolas municipality (Eckert et al., 2010b; Gaucher et al., 2009), could be reconstructed with the highest level of confidence on paths E1, C1, and C2. On C1 and C2, the absence of EPA records renders a comparison impossible. On paths E1 and E2, the convergence rate between the EPA and the tree-ring reconstruction significantly exceeds those reported by previous studies made in the French Alps by Corona et al. (2012, 43%), Corona et al. (2013, 43%), Schläppy et al. (2013, 38%) and Schläppy et al. (2014, 33-45%). This synchronicity confirms the potential of forested avalanche paths for a detailed reconstruction of past avalanche activity. Albeit the fact that GDs were observed in tree-ring series in 1947 (14), 1951 (8), and 1986 (8), these events listed in historical records were not confirmed with dendrogeomorphic analysis as the It, GD, or Wit values did not exceed the required thresholds. This lack may be attributed to the stringency of the procedure employed here, designed to limit the introduction of noise but could equally be related to an over-sensibility of the dendrogeomorphic approach. Indeed, one should indeed keep in mind that the It, GD, and Wit thresholds used in the first and third steps are empirical. As no consensus exist in literature, they have been synthesized from Corona et al. (2014), Favillier et al. (2017), Kogelnig-Mayer et al. (2011) and Schneuwly-Bollschweiler et al. (2013) but cannot be considered as absolute values suitable for all sites. Similarly, in the second step, the threshold of four mechanical disturbances was arbitrary chosen to disentangle snow avalanche events from climate and larch budmoth outbreaks (Favillier et al., 2017) and may therefore lead to the omission of minor events and to an underestimation of past avalanche activity. In addition, (i) snow avalanches reported in historical chronicles have to be of sufficient magnitude to have impacts on trees, but (ii) not too major as they would then destroy large parts of the forest stand and thereby remove evidence of past and subsequent events or disturb tree growth in such a way that younger events cannot be identified in the tree-ring record (e.g. Carrara, 1979; Kogelnig-Mayer et al., 2011). As a consequence, and despite our high success rate, the number of reconstructed events has to be seen as a minimum frequency of natural avalanche activity.

5.2. Two different avalanche dynamics

In this study, we deliberately chose contiguous avalanche paths with different morphometric characteristics and forest cover, with the aim to detect differences in their potential to record past events in trees. On the one hand, paths E1 and E2 are characterized by forested release areas, located at altitudes <2340 m asl and the presence of a very dense shrub cover (mainly *R. ferrugineum*), with an average height of about 0.70 m. Both paths have limited areas (<25ha), their length does not exceed 1000 m, and they are almost completely covered by open larch stands. On the other hand, on paths C1 and C2, snow avalanches are commonly triggered naturally from unforested release zones located above 2290 m asl and covered by shrubby grassland. Their lengths exceed 1500 m and they show a marked transverse vegetation zonation (Malanson and Butler, 1986) with an inner zone

colonized by shrubs and shade-intolerant pioneer tree species and forest vegetation (mainly European larch) in the outer zone. The performed snow avalanche simulations reveal that maximum velocities and maximum pressures are significantly higher in these paths than on paths E1 and E2.

As expected, avalanche dynamics strongly differ from C1/C2 to E1/E2. On paths C1 and C2, all snow avalanches reach the lower sections of the slope and are reconstructed with a high level of confidence. Avalanches in paths C1 and C2 are often accompanied by large forest removal, such as in the 1960s and after 2009 according to archival documents, and reveal the intense and destructive nature of snow avalanches in these paths. Paradoxically, the recurrence intervals calculated on path C1 (24 years over the period 1961-2009) and C2 (23 years over the period 1894-2009) are much lower than those calculated for paths E1 and E2. This paradox can neither be explained by path characteristics nor by the vegetation structure that could plead for a higher frequency of snow avalanches on paths C1 and C2. By contrast, we can reasonably hypothesize that they result from a gap in the dendrogeomorphic approach. More explicitly, it is likely that the periodic destruction of the forest stands by high-magnitude snow avalanches, comparable to those observed in 1962 or 2009, jointly limits the length of the reconstruction as well as the number of the reconstructed events (Corona et al., 2012). In addition, despite the presence of multi-century-old larch trees along the outer margins of both paths, no avalanches could be reconstructed prior to the end of the 19th century, thus suggesting that the lateral extents of snow avalanches during the Little Ice Age did not exceed those of the 20th century.

On the contrary, on paths E1 and E2, the reconstructions derived from tree-ring analyses span longer periods (1791-2016 and 1809-1998, respectively), and exceed those derived for paths C1 and C2 by more than one century. Comparable decadal avalanche recurrence intervals, 2.5 times higher than on paths C1/C2, are reconstructed on paths E1/E2. We assume that the intensity of past avalanche events has been more moderate. This assumption is supported by a vast body of evidence such as (1) the lower altitude of vegetated release areas, (2) higher forest coverage, (3) the output of the RAMMS simulations, (4) the presence of older trees, (5) the diachronic analysis of aerials photographs showing only limited changes in forest cover, and (6) more heterogeneous runout distances with 29, 46, and 25% of the reconstructed event reaching the upper, medium, and lower sampling transects, respectively.

These results have strong implications for dendrogeomorphic studies. Indeed, to evidence the potential impacts of global warming on snow avalanches, tree-ring reconstructions aim at investigating snow avalanche–climate linkages (Casteller et al., 2011; Decaulne et al., 2014; Dubé et al., 2004; Gądek et al., 2017; Germain et al., 2009, 2005; Hebertson and Jenkins, 2003; Martin and Germain, 2017, 2016; Muntán et al., 2009; Schläppy et al., 2016; Voiculescu et al., 2016) and at comparing current activity with colder periods such as the Little Ice Age (see e.g., Ballesteros-Cánovas et al., 2018; Corona et al., 2013; Giacona et al., 2018). These studies generally focus on

long-lived stands and should rely on reconstructions that are as complete and continuous as possible. In this context, our study confirms that a careful selection of avalanche paths is a very critical prerequisite as it conditions both the length and the reliability of the reconstructions. In detail, it shows the great potential of forested slopes affected by snow avalanches of low to medium magnitudes, as they have the best boundary conditions to yield comprehensive, long-range reconstructions that can then be used for the detection of climate-driven trends or shifts. Although we are aware that our approach does not cover the entire avalanche regime (i.e. from very small to extremely large events), these results are all the more interesting as avalanche activity on these paths is more susceptible to be strongly affected by global warming as (1) warmer winter temperatures and decreasing days with a minimum snow depth required for avalanches will probably further reduce the importance of avalanche disturbances in forested terrain in the future (Castebrunet et al., 2014) and (2) warmer temperature during the growing season will probably further facilitate forest expansion and productivity (Bebi et al., 2009) at these sites. One should yet keep in mind that these recommendations are strictly focused on comprehensiveness of all avalanches, regardless of whether they represent a hazard or not, and that the time-consuming sampling methodology presented here, may not be necessary or appropriate for locations where the priority is on identifying the largest magnitude, most hazardous snow avalanches that cause the greatest impacts to people and infrastructure.

6. Conclusions

In this study, a dendrogeomorphic approach has been used to reconstruct past avalanche activity on four contiguous paths located in the upper Guil valley (Queyras massif, French Alps), and characterized by different structures and forest covers. In total, 306 *Larix decidua* Mill. trees were sampled along three altitudinal transects to reconstruct 52 avalanche events. Despite the fact that several limitations may persist in terms of the arbitrary thresholds chosen for the detection of events and the exclusion of noise from reconstructions, our results show very different avalanche dynamics in different avalanche couloirs of the same slope. Unsurprisingly, on paths C1 and C2, characterized by high-altitude release areas that are only covered by shrubby vegetation, high-magnitude events reach the lower transect and cause damage to the forest stand. By contrast, on paths E1 and E2, a forest cover up to the release areas limits the intensity and the spatial extent of past events. More interestingly, the frequency of events reconstructed on the latter paths is 2.5 times higher, reconstructions cover a longer time span and the convergence rate with events listed in the EPA archive attests clearly to the reliability of the reconstructed avalanche history. These results have particularly important implications for avalanche reconstructions aiming at deciphering avalanche activity fluctuations in the current context of global warming. They suggest that a careful selection of the couloirs is essential and that a priority should be given to forested paths since (i) they allow for exhaustive and (ii) reliable reconstructions over (iii) long periods of time.

Acknowledgment

The authors wish to address special thanks to Ana Casado, Loïc Francon, Pauline Morel, Louis Sembel and Taline Zgheib for their assistance on the field. This work was supported by Université Grenoble Alpes with the grant “RARETES” (avalanche risk as revealer of long-range interactions between environment and society, AGIR-PEPS 2016 program); and the French government IDEX-ISITE initiative 16-IDEX-0001 (CAP 20-25). Irstea is a member of Labex OSUG@2020. The authors acknowledge insightful feedback from the referees and the handling editor Elena Paoletti.

References

Alestalo, J., 1971. Dendrochronological interpretation of geomorphic processes. Fennia 1–139.

ARPA, CEMAGREF, 2008. Projet n°165 PROVIALP : Protection de la Viabilité Alpine - Rapport Final (Rapport Final). ARPA, CEMAGREF, Torino (Ita).

Ballesteros-Cánovas, J.A., Trappmann, D., Madrigal-González, J., Eckert, N., Stoffel, M., 2018. Climate warming enhances snow avalanche risk in the Western Himalayas. Proc. Natl. Acad. Sci. 201716913. https://doi.org/10.1073/pnas.1716913115

Baltensweiler, W., Benz, G., Bovey, P., Delucchi, V., 1977. Dynamics of Larch Bud Moth Populations. Annu. Rev. Entomol. 22, 79–100. https://doi.org/10.1146/annurev.en.22.010177.000455

Bartelt, P., Stöckli, V., 2001. The influence of tree and branch fracture, overturning and debris entrainment on snow avalanche flow. Ann. Glaciol. 32, 209–216. https://doi.org/10.3189/172756401781819544

Bebi, P., Kulakowski, D., Rixen, C., 2009. Snow avalanche disturbances in forest ecosystems—State of research and implications for management. For. Ecol. Manag., Disturbances in Mountain Forests: Implications for Management 257, 1883–1892. https://doi.org/10.1016/j.foreco.2009.01.050

Bollschweiler, M., Stoffel, M., Schneuwly, D.M., 2008a. Dynamics in debris-flow activity on a forested cone — A case study using different dendroecological approaches. CATENA 72, 67–78. https://doi.org/10.1016/j.catena.2007.04.004

Bollschweiler, M., Stoffel, M., Schneuwly, D.M., Bourqui, K., 2008b. Traumatic resin ducts in Larix decidua stems impacted by debris flows. Tree Physiol. 28, 255–263. https://doi.org/10.1093/treephys/28.2.255

Bonnefoy, M., Barral, L., Cabos, S., Escande, S., Gaucher, R., Pasquier, X., Richard, D., 2010. The localization map of avalanche phenomena (CLPA): Stakes and prospects. Proc. 2010 Int. Snow Sci. Workshop Squaw Valley Cal. 699–705.

Boucher, D., Filion, L., Hétu, B., 2003. Reconstitution dendrochronologique et fréquence des grosses avalanches de neige dans un couloir subalpin du mont Hog’s Back, en Gaspésie centrale (Québec). Géographie Phys. Quat. 57, 159–168. https://doi.org/10.7202/011311ar

Bourova, E., Maldonado, E., Leroy, J.-B., Alouani, R., Eckert, N., Bonnefoy-Demongeot, M., Deschatres, M., 2016. A new web-based system to improve the monitoring of snow avalanche hazard in France. Nat. Hazards Earth Syst. Sci. 16, 1205–1216. https://doi.org/10.5194/nhess-16-1205-2016

Bründl, M., Etter, H.-J., Steiniger, M., Klingler, C., Rhyner, J., Ammann, W.J., 2004. IFKIS - a basis for managing avalanche risk in settlements and on roads in Switzerland. Nat. Hazards Earth Syst. Sci. 4, 257–262.

Bryant, C.L., Butler, D.R., Vitek, J.D., 1989. A statistical analysis of tree-ring dating in conjunction with snow avalanches: Comparison of on-path versus off-path responses. Environ. Geol. Water Sci. 14, 53–59. https://doi.org/10.1007/BF01740585

Burrows, C.J., Burrows, V.L., 1976. Procedures for the study of snow avalanche chronology using growth layers of woody plants: Boulder, Colorado. Inst. Arct. Alp. Res. Occasional Paper, 54p.

Butler, D.R., 1979. Snow Avalanche Path Terrain and Vegetation, Glacier National Park, Montana. Arct. Alp. Res. 11, 17–32. https://doi.org/10.2307/1550456

Butler, D.R., Malanson, G.P., 1985. A Reconstruction of Snow-Avalanche Characteristics in Montana, U.S.A., Using Vegetative Indicators. J. Glaciol. 31, 185–187. https://doi.org/10.3189/S0022143000006444

Butler, D.R., Sawyer, C.F., 2008. Dendrogeomorphology and high-magnitude snow avalanches: a review and case study. Nat. Hazards Earth Syst. Sci. 8, 303–309. https://doi.org/10.5194/nhess-8-303-2008

Butler, D.R., Sawyer, C.F., Maas, J.A., 2010. Tree-ring dating of snow avalanches in Glacier National Park, Montana, USA, in: Stoffel, M., Bollschweiler, M., Butler, D.R., Luckman, B.H. (Eds.), Tree Rings and Natural Hazards - A State-of-the-Art. Springer, Dordrecht, pp. 33–44.

Carrara, P.E., 1979. The determination of snow avalanche frequency through tree-ring analysis and historical records at Ophir, Colorado. Geol. Soc. Am. Bull. 90, 773–780. https://doi.org/10.1130/0016-7606(1979)90<773:TDOSAF>2.0.CO;2

Castebrunet, H., Eckert, N., Giraud, G., Durand, Y., Morin, S., 2014. Projected changes of snow conditions and avalanche activity in a warming climate: a case study in the French Alps over the 2020–2050 and 2070–2100 periods. Cryosphere Discuss 8, 581–640. https://doi.org/10.5194/tcd-8-581-2014

Casteller, A., Christen, M., Villalba, R., Martínez, H., Stöckli, V., Leiva, J.C., Bartelt, P., 2008. Validating numerical simulations of snow avalanches using dendrochronology: the Cerro Ventana event in Northern Patagonia, Argentina. Nat. Hazards Earth Syst. Sci. 8, 433–443. https://doi.org/10.5194/nhess-8-433-2008

Casteller, A., Stöckli, V., Villalba, R., Mayer, A.C., 2007. An Evaluation of Dendroecological Indicators of Snow Avalanches in the Swiss Alps. Arct. Antarct. Alp. Res. 39, 218–228. https://doi.org/10.1657/1523-0430(2007)39[218:AEODIO]2.0.CO;2

Casteller, A., Villalba, R., Araneo, D., Stöckli, V., 2011. Reconstructing temporal patterns of snow avalanches at Lago del Desierto,southern Patagonian Andes. Cold Reg. Sci. Technol. 67, 68–78. https://doi.org/10.1016/j.coldregions.2011.02.001

Christen, M., Kowalski, J., Bartelt, P., 2010. RAMMS: Numerical simulation of dense snow avalanches in three-dimensional terrain. Cold Reg. Sci. Technol. 63, 1–14. https://doi.org/10.1016/j.coldregions.2010.04.005

Corona, C., Lopez Saez, J., Stoffel, M., 2014. Defining optimal sample size, sampling design and thresholds for dendrogeomorphic landslide reconstructions. Quat. Geochronol. 22, 72–84. https://doi.org/10.1016/j.quageo.2014.02.006

Corona, C., Lopez Saez, J., Stoffel, M., Bonnefoy, M., Richard, D., Astrade, L., Berger, F., 2012. How much of the real avalanche activity can be captured with tree rings? An evaluation of classic dendrogeomorphic approaches and comparison with historical archives. Cold Reg. Sci. Technol. 74–75, 31–42. https://doi.org/10.1016/j.coldregions.2012.01.003

Corona, C., Rovéra, G., Lopez Saez, J., Stoffel, M., Perfettini, P., 2010. Spatio-temporal reconstruction of snow avalanche activity using tree rings: Pierres Jean Jeanne avalanche talus, Massif de l'Oisans, France. Catena 83, 107–118. https://doi.org/10.1016/j.catena.2010.08.004

Corona, C., Saez, J.L., Stoffel, M., Rovéra, G., Edouard, J.-L., Berger, F., 2013. Seven centuries of avalanche activity at Echalp (Queyras massif, southern French Alps) as inferred from tree rings. The Holocene 23, 292–304. https://doi.org/10.1177/0959683612460784

Decaulne, A., Eggertsson, Ó., Laute, K., Beylich, A.A., 2014. A 100-year extreme snow-avalanche record based on tree-ring research in upper Bødalen, inner Nordfjord, western Norway. Geomorphology 218, 3–15. https://doi.org/10.1016/j.geomorph.2013.12.036

Dubé, S., Filion, L., Hétu, B., 2004. Tree-Ring Reconstruction of High-Magnitude Snow Avalanches in the Northern Gaspé Peninsula, Québec, Canada. Arct. Antarct. Alp. Res. 36, 555–564.

Eckert, N., Parent, E., Belanger, L., Garcia, S., 2007. Hierarchical modelling for spatial analysis of the number of avalanche occurrences at the scale of the township. Cold Regions Science and Technology 50. pp 97-112. https://doi.org/10.1016/j.coldregions.2007.01.008

Eckert, N., Parent, E., Kies, R., Baya, H., 2010a. A spatio-temporal modelling framework for assessing the fluctuations of avalanche occurrence resulting from climate change: application to 60 years of data in the northern French Alps. Climatic Change. Vol. 101, N° 3-4. pp 515-553. https://doi.org/10.1007/s10584-009-9718-8

Eckert, N., Coleou, C., Castebrunet, H., Giraud, G., Deschatres, M., Gaume, J., 2010b. Cross-comparison of meteorological and avalanche data for characterising avalanche cycles: the example of December 2008 in the eastern part of the French Alps. Cold Reg. Sci. Technol. 64, 119–136. https://doi.org/10.1016/j.coldregions.2010.08.009

518 Efthymiadis, D., Jones, P.D., Briffa, K.R., Auer, I., Böhm, R., Schöner, W., Frei, C., Schmidli, J., 2006.
519 Construction of a 10-min-gridded precipitation data set for the Greater Alpine Region for 1800–2003. J.
520 Geophys. Res. 111. https://doi.org/10.1029/2005JD006120
521 Einhorn, B., Eckert, N., Chaix, C., Ravanel, L., Deline, P., Gardent, M., Boudières, V., Richard, D., Vengeon, J.-
522 M., Giraud, G., Schoeneich, P., 2015. Changements climatiques et risques naturels dans les Alpes:
523 Impacts observés et potentiels sur les systèmes physiques et socio-économiques. Rev. Géographie Alp.
524 https://doi.org/10.4000/rga.2829
525 ESRI, 2013. ArcGIS 10.2.1. ESRI, Redlands, CA.
526 Favillier, A., Guillet, S., Morel, P., Corona, C., Lopez-Saez, J., Eckert, N., Ballesteros Cánovas, J.A., Peiry, J.-L.,
527 Stoffel, M., 2017. Disentangling the impacts of exogenous disturbances on forest stands to assess multi-
528 centennial tree-ring reconstructions of avalanche activity in the upper Goms Valley (Canton of Valais,
529 Switzerland). Quat. Geochronol. 42, 89–104. https://doi.org/10.1016/j.quageo.2017.09.001
530 Favillier, A., Guillet, S., Trappmann, D., Morel, P., Lopez-Saez, J., Eckert, N., Zenhäusern, G., Peiry, J.-L., Stoffel,
531 M., Corona, C., 2018. Spatio-temporal maps of past avalanche events derived from tree-ring analysis: A
532 case study in the Zermatt valley (Valais, Switzerland). Cold Reg. Sci. Technol. 154, 9–22.
533 https://doi.org/10.1016/j.coldregions.2018.06.004
534 Gądek, B., Kaczka, R.J., Rączkowska, Z., Rojan, E., Casteller, A., Bebi, P., 2017. Snow avalanche activity in Żleb
535 Żandarmerii in a time of climate change (Tatra Mts., Poland). CATENA 158, 201–212.
536 https://doi.org/10.1016/j.catena.2017.07.005
537 Garavaglia, V., Pelfini, M., 2011. The role of border areas for dendrochronological investigations on catastrophic
538 snow avalanches: A case study from the Italian Alps. CATENA 87, 209–215.
539 https://doi.org/10.1016/j.catena.2011.06.006
540 Gaucher, R., Pasquier, X., Bonnefoy, M., Eckert, N., Deschatres, M., 2009. Quelques exemples d'avalanches
541 exceptionelles. Neige Avalanche 10–14.
542 Gaume J., Eckert, N., Chambon G., Eckert N., Naaim M., Bel, L., 2013. Mapping extreme snowfalls in the French
543 Alps using Max-Stable processes. Water Resources Research. Volume 49, Issue 2, pp 1079–1098.
544 https://doi.org/10.1002/wrcr.20083
545 Germain, D., Filion, L., Hétu, B., 2009. Snow avalanche regime and climatic conditions in the Chic-Choc Range,
546 eastern Canada. Clim. Change 92, 141–167. https://doi.org/10.1007/s10584-008-9439-4
547 Germain, D., Filion, L., Hétu, B., 2005. Snow avalanche activity after fire and logging disturbances, northern
548 Gaspé Peninsula, Quebec, Canada. Can. J. Earth Sci. 42, 2103–2116. https://doi.org/10.1139/e05-087
549 Giacona, F., Eckert, N., Mainieri, R., Martin, B., Corona, C., Lopez-Saez, J., Monnet, J.-M., Naaim, M., Stoffel, M.,
550 2018. Avalanche activity and socio-environmental changes leave strong footprints in forested

551 landscapes: a case study in the Vosges medium-high mountain range. Ann. Glaciol. 1–23.
552 https://doi.org/10.1017/aog.2018.26
553 Gobiet, A., Kotlarski, S., Beniston, M., Heinrich, G., Rajczak, J., Stoffel, M., 2014. 21st century climate change in
554 the European Alps—A review. Sci. Total Environ. 493, 1138–1151.
555 https://doi.org/10.1016/j.scitotenv.2013.07.050
556 Gruber, U., Bartelt, P., 2007. Snow avalanche hazard modelling of large areas using shallow water numerical
557 methods and GIS. Environ. Model. Softw. 22, 1472–1481. https://doi.org/10.1016/j.envsoft.2007.01.001
558 Hebertson, E.G., Jenkins, M.J., 2003. Historic climate factors associated with major avalanche years on the
559 Wasatch Plateau, Utah. Cold Reg. Sci. Technol. 37, 315–332. https://doi.org/10.1016/S0165-
560 232X(03)00073-9
561 Heffernan, O., 2018. Coming down the tracks. Nat. Clim. Change 8, 937–939. https://doi.org/10.1038/s41558-
562 018-0306-7
563 Jamard, A.L., Garcia, S., Bélanger, L., 2002. L'enquête permanente sur les Avalanches (EPA). Statistique
564 descriptive générale des événements et des sites. (DESS Ingéniérie Mathématique option Statistique.).
565 Université Joseph Fourrier, Grenoble, France.
566 Kennedy, M., 2013. Introducing geographic information systems with ArcGIS: a workbook approach to learning
567 GIS, Third edition. ed. John Wiley & Sons, Hoboken, New Jersey.
568 Kogelnig-Mayer, B., Stoffel, M., Schneuwly-Bollschweiler, M., 2013. Four-dimensional growth response of mature
569 Larix decidua to stem burial under natural conditions. Trees 27, 1217–1223.
570 https://doi.org/10.1007/s00468-013-0870-4
571 Kogelnig-Mayer, B., Stoffel, M., Schneuwly-Bollschweiler, M., Hübl, J., Rudolf-Miklau, F., 2011. Possibilities and
572 Limitations of Dendrogeomorphic Time-Series Reconstructions on Sites Influenced by Debris Flows and
573 Frequent Snow Avalanche Activity. Arct. Antarct. Alp. Res. 43, 649–658. https://doi.org/10.1657/1938-
574 4246-43.4.649
575 Kress, A., Saurer, M., Büntgen, U., Treydte, K.S., Bugmann, H., Siegwolf, R.T.W., 2009. Summer temperature
576 dependency of larch budmoth outbreaks revealed by Alpine tree-ring isotope chronologies. Oecologia
577 160, 353–365. https://doi.org/10.1007/s00442-009-1290-4
578 Laxton, S.C., Smith, D.J., 2009. Dendrochronological reconstruction of snow avalanche activity in the Lahul
579 Himalaya, Northern India. Nat. Hazards 49, 459–467. https://doi.org/10.1007/s11069-008-9288-5
580 Lemoine, M., Tricart, P., 1986. Les Schistes lustrés des Alpes occidentales: Approche stratigraphique, structurale
581 et sédimentologique. Eclogae Geol. Helvetiae 79, 271–294.
582 Malanson, G.P., Butler, D.R., 1986. Floristic Patterns on Avalanche Paths in the Northern Rocky Mountains, Usa.
583 Phys. Geogr. 7, 231–238. https://doi.org/10.1080/02723646.1986.10642293

584 Martin, J.-P., Germain, D., 2017. Large-scale teleconnection patterns and synoptic climatology of major snow-
585 avalanche winters in the Presidential Range (New Hampshire, USA). Int. J. Climatol. 37, 109–123.
586 https://doi.org/10.1002/joc.4985
587 Martin, J.-P., Germain, D., 2016. Dendrogeomorphic reconstruction of snow avalanche regime and triggering
588 weather conditions A classification tree model approach. Prog. Phys. Geogr. 40, 0309133315625863.
589 https://doi.org/10.1177/0309133315625863
590 Mears, A.I., 1975. Dynamics of dense-snow avalanches interpreted from broken trees. Geology 3, 521.
591 https://doi.org/10.1130/0091-7613(1975)3<521:DODAIF>2.0.CO;2
592 Mougin, P., 1922. Les avalanches en Savoie. Ministère de l'Agriculture, Direction Générale des Eaux et Forêts,
593 Service des Grandes Forces Hydrauliques, Paris.
594 Muntán, E., Andreu, L., Oller, P., Gutiérrez, E., Martínez, P., 2004. Dendrochronological study of the Canal del
595 Roc Roig avalanche path: first results of the Aludex project in the Pyrenees. Ann. Glaciol. 38, 173–179.
596 https://doi.org/10.3189/172756404781815077
597 Muntán, E., García, C., Oller, P., Martí, G., García, A., Gutiérrez, E., 2009. Reconstructing snow avalanches in
598 the Southeastern Pyrenees. Nat. Hazards Earth Syst. Sci. 9, 1599–1612. https://doi.org/10.5194/nhess-
599 9-1599-2009
600 Nöthiger, C., Elsasser, H., 2004. Natural Hazards and Tourism: New Findings on the European Alps. Mt. Res.
601 Dev. 24, 24–27. https://doi.org/10.1659/0276-4741(2004)024[0024:NHATNF]2.0.CO;2
602 Potter, N., 1969. Tree-Ring Dating of Snow Avalanche Tracks and the Geomorphic Activity of Avalanches,
603 Northern Absaroka Mountains, Wyoming. Geol. Soc. Am. Spec. Pap. 123, 141–166.
604 https://doi.org/10.1130/SPE123-p141
605 Rudolf-Miklau, F., Sauermoser, S., Mears, A.I., Boensch, M.M., 2015. The technical avalanche protection
606 handbook. ed. John Wiley & Sons, Berlin, Germany.
607 Salm, B., 1982. Mechanical properties of snow. Rev. Geophys. 20, 1–19.
608 https://doi.org/10.1029/RG020i001p00001
609 Saulnier, M., Roques, A., Guibal, F., Rozenberg, P., Saracco, G., Corona, C., Edouard, J.-L., 2017.
610 Spatiotemporal heterogeneity of larch budmoth outbreaks in the French Alps over the last 500 years.
611 Can. J. For. Res. 47, 667–680. https://doi.org/10.1139/cjfr-2016-0211
612 Schläppy, R., Eckert, N., Jomelli, V., Stoffel, M., Grancher, D., Brunstein, D., Naaim, M., Deschatres, M., 2014.
613 Validation of extreme snow avalanches and related return periods derived from a statistical-dynamical
614 model using tree-ring techniques. Cold Reg. Sci. Technol. 99, 12–26.
615 https://doi.org/10.1016/j.coldregions.2013.12.001

Schläppy, R., Jomelli, V., Eckert, N., Stoffel, M., Grancher, D., Brunstein, D., Corona, C., Deschatres, M., 2016. Can we infer avalanche–climate relations using tree-ring data? Case studies in the French Alps. Reg. Environ. Change 16, 629–642. https://doi.org/10.1007/s10113-015-0823-0

Schläppy, R., Jomelli, V., Grancher, D., Stoffel, M., Corona, C., Brunstein, D., Eckert, N., Deschatres, M., 2013. A New Tree-Ring-Based, Semi-Quantitative Approach for the Determination of Snow Avalanche Events: use of Classification Trees for Validation. Arct. Antarct. Alp. Res. 45, 383–395. https://doi.org/10.1657/1938-4246-45.3.383

Schneuwly, D.M., Stoffel, M., Bollschweiler, M., 2009a. Formation and spread of callus tissue and tangential rows of resin ducts in Larix decidua and Picea abies following rockfall impacts. Tree Physiol. 29, 281–289. https://doi.org/10.1093/treephys/tpn026

Schneuwly, D.M., Stoffel, M., Dorren, L.K.A., Berger, F., 2009b. Three-dimensional analysis of the anatomical growth response of European conifers to mechanical disturbance. Tree Physiol. 29, 1247–1257. https://doi.org/10.1093/treephys/tpp056

Schneuwly-Bollschweiler, M., Corona, C., Stoffel, M., 2013. How to improve dating quality and reduce noise in tree-ring based debris-flow reconstructions. Quat. Geochronol. 18, 110–118. https://doi.org/10.1016/j.quageo.2013.05.001

Schweizer, J., 2003. Snow avalanche formation. Rev. Geophys. 41. https://doi.org/10.1029/2002RG000123

Shroder, J.F., 1980. Dendrogeomorphology: review and new techniques of tree-ring dating. Prog. Phys. Geogr. 4, 161–188. https://doi.org/10.1177/030913338000400202

Shroder, J.F., 1978. Dendrogeomorphological Analysis of Mass Movement on Table Cliffs Plateau, Utah. Quat. Res. 9, 168–185. https://doi.org/10.1016/0033-5894(78)90065-0

Šilhán, K., Stoffel, M., 2015. Impacts of age-dependent tree sensitivity and dating approaches on dendrogeomorphic time series of landslides. Geomorphology 236, 34–43. https://doi.org/10.1016/j.geomorph.2015.02.003

Stoffel, M., Bollschweiler, M., 2008. Tree-ring analysis in natural hazards research, an overview. Nat. Hazards Earth Syst. Sci. 8, 187–202. https://doi.org/10.5194/nhess-8-187-2008

Stoffel, M., Bollschweiler, M., Butler, D.R., Luckman, B.H., 2010. Tree rings and natural hazards: A State-of-the-Art. Springer, Dordrecht, New York.

Stoffel, M., Bollschweiler, M., Hassler, G.-R., 2006. Differentiating past events on a cone influenced by debris-flow and snow avalanche activity – a dendrogeomorphological approach. Earth Surf. Process. Landf. 31, 1424–1437. https://doi.org/10.1002/esp.1363

Stoffel, M., Butler, D.R., Corona, C., 2013. Mass movements and tree rings: A guide to dendrogeomorphic field sampling and dating. Geomorphology 200, 106–120. https://doi.org/10.1016/j.geomorph.2012.12.017

649 Stoffel, M., Corona, C., 2018. Future winters glimpsed in the Alps. Nat. Geosci. 11, 458–460.
650 https://doi.org/10.1038/s41561-018-0177-6
651 Stoffel, M., Corona, C., 2014. Dendroecological Dating of Geomorphic Disturbance in Trees. Tree-Ring Res. 70,
652 3–20. https://doi.org/10.3959/1536-1098-70.1.3
653 Stoffel, M., Hitz, O.M., 2008. Rockfall and snow avalanche impacts leave different anatomical signatures in tree
654 rings of juvenile Larix decidua. Tree Physiol. 28, 1713–1720. https://doi.org/10.1093/treephys/28.8.1713
655 Stoffel, M., Perret, S., 2006. Reconstructing past rockfall activity with tree rings: Some methodological
656 considerations. Dendrochronologia 1–15.
657 Techel, F., Jarry, F., Kronthaler, G., Mitterer, S., Nairz, P., Pavšek, M., Valt, M., Darms, G., 2016. Avalanche
658 fatalities in the European Alps: long-term trends and statistics. Geogr. Helvetica 71, 147–159.
659 https://doi.org/10.5194/gh-71-147-2016
660 Teich, M., Bartelt, P., Grêt-Regamey, A., Bebi, P., 2012. Snow Avalanches in Forested Terrain: Influence of
661 Forest Parameters, Topography, and Avalanche Characteristics on Runout Distance. Arct. Antarct. Alp.
662 Res. 44, 509–519. https://doi.org/10.1657/1938-4246-44.4.509
663 Tichavský, R., Šilhán, K., 2016. The changing ability of Norway spruce (P. abies) to record hydro-geomorphic
664 processes based on the age and diameter of the tree stem – A dendrogeomorphic approach. CATENA
665 147, 469–480. https://doi.org/10.1016/j.catena.2016.07.052
666 Timell, T.E., 1986. Compression wood in gymnosperms. Springer, Berlin.
667 Touflan, P., Talon, B., Walsh, K., 2010. Soil charcoal analysis: a reliable tool for spatially precise studies of past
668 forest dynamics: a case study in the French Southern Alps. The Holocene 20, 45–52.
669 https://doi.org/10.1177/0959683609348900
670 Trappmann, D., Corona, C., Stoffel, M., 2013. Rolling stones and tree rings: A state of research on
671 dendrogeomorphic reconstructions of rockfall. Prog. Phys. Geogr. 37, 701–716.
672 https://doi.org/10.1177/0309133313506451
673 Van der Burght, L., Stoffel, M., Bigler, C., 2012. Analysis and modelling of tree succession on a recent rockslide
674 deposit. Plant Ecol. 213, 35–46. https://doi.org/10.1007/s11258-011-0004-2
675 Voiculescu, M., Onaca, A., Chiroiu, P., 2016. Dendrogeomorphic reconstruction of past snow avalanche events in
676 Bâlea glacial valley–Făgăraş massif (Southern Carpathians), Romanian Carpathians. Quat. Int. 415,
677 286–302. https://doi.org/10.1016/j.quaint.2015.11.115

678

679

680

Captions

Figure 1. Location of the study site in the Guil valley (Queyras massif, French Alps) (a) and delineation of the four avalanche paths on the Ravin de la Salce slope (b).

Figure 2. Synoptic diagram of the 4-step approach used for the detection of avalanche events in tree-ring series, adapted from Favillier et al. (2017).

Figure 3. (a) Maximum velocities and (b) maximum pressures computed with the RAMMS snow avalanche model. Avalanche extensions obtained with RAMMS are used in this study to delineate avalanche paths E1-C2.

Figure 4. Age structure of the forest stand growing at the Ravin de la Salce slope.

Figure 5. Event-response histograms showing the total number of growth disturbances (GD, in red and orange) and the percentage of trees responding to an event (in green) at each of the four paths. Orange bars show the total number of growth reductions which are possibly related to larch budmoth outbreaks or to climatic extremes. The dashed lines denote the GD and It thresholds used to reconstruct past avalanche events. The solid lines denote sample depth, i.e. the number of trees available for analysis for each year of the reconstruction.

Figure 6. Results of the 4-step procedure. Reconstructed event characteristics take into account possible interference with climate or larch budmoth outbreaks, and include the level of confidence and the minimum slide extent.

Figure 7. Avalanche events reconstructed for the period 1720-2016 at the four avalanche paths. Symbol sizes are proportional to the level of confidence, whereas the color range denotes the minimum slide extent. Grey bands represent years associated to LBM outbreaks. Vertical lines show snow avalanche events documented in historical archives (black), as well as extremely dry (orange), cold (blue) summers and pointer years (green).

Figure 8. Location of trees disturbed in 1961 and 2008 and presumably corresponding to avalanches that occurred (c) on February 7, 1961 and (f) on December 17, 2008 and diachronic comparisons of aerial photographs (IGN) highlighting the evolution of the forest stand between 1956 and 1962 (a, b) and between 1988 and 2009 (d,e).

Table 1. Larch budmoth events and pointer years (according to Saulnier et al., 2017), as well as extremely cold and dry summers (Efthymiadis et al., 2006) in the French Alps. All these years have been carefully analyzed due to probable interferences between snow avalanche damage in trees, as well as LBM and climatic signals that may induce growth reductions comparable to those observed after snow avalanches in the tree-ring series.

Table 2. Geomorphic characteristics and soil occupation of the studied avalanche paths and their release zones.

710 Table 3. Intensity of reactions and types of growth disturbances (GD) assessed in the 306 larch trees selected for
711 analysis.

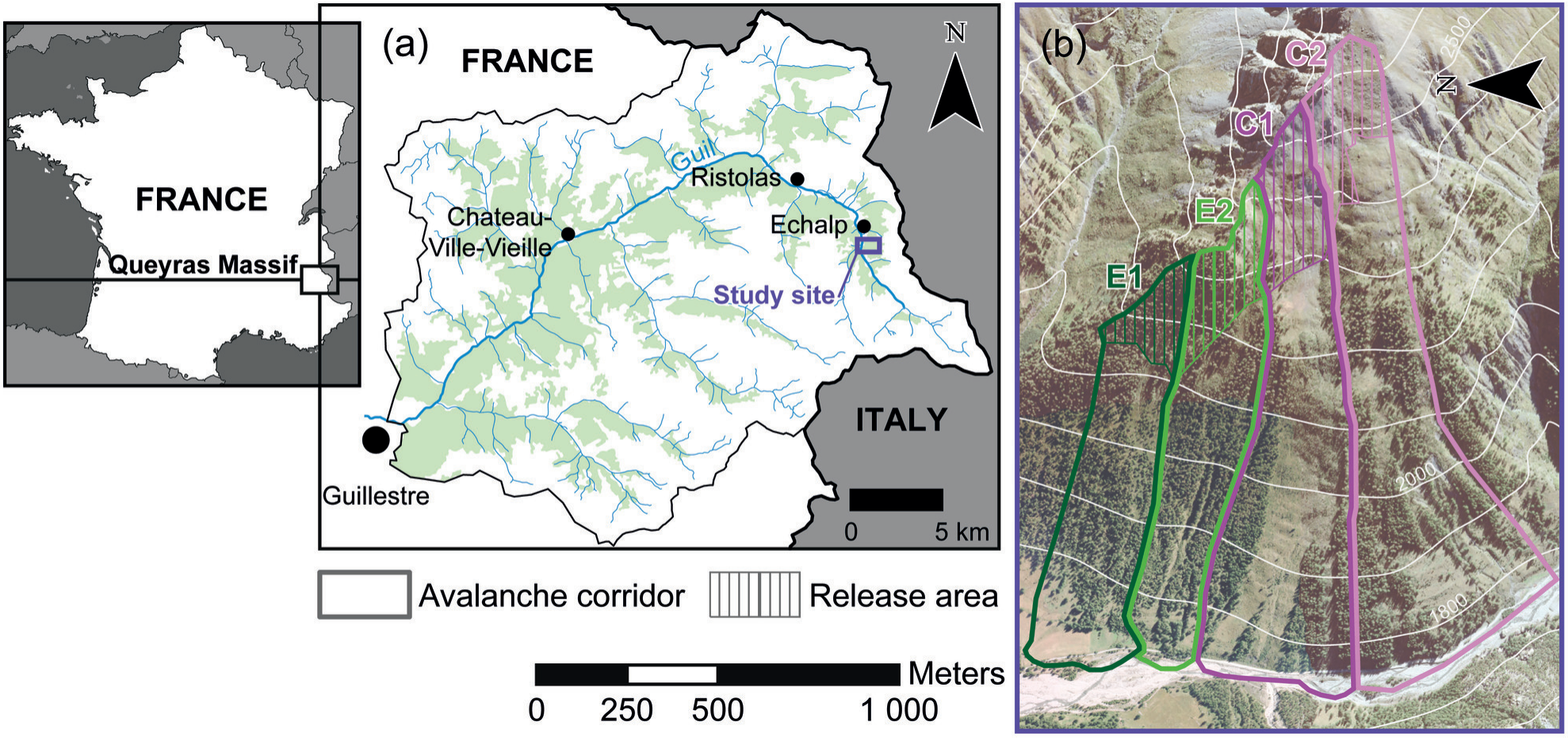
FRANCE
Queyras Massif
(a)
FRANCE
N
Guil
Ristolas
Chateau-
Ville-Vieille
Echalp
Study site
ITALY
Guillestre
0
5 km
Avalanche corridor
Release area
Meters
0
250
500
1 000
(b)
C2
C1
E2
E1
N
2500
2000
1800

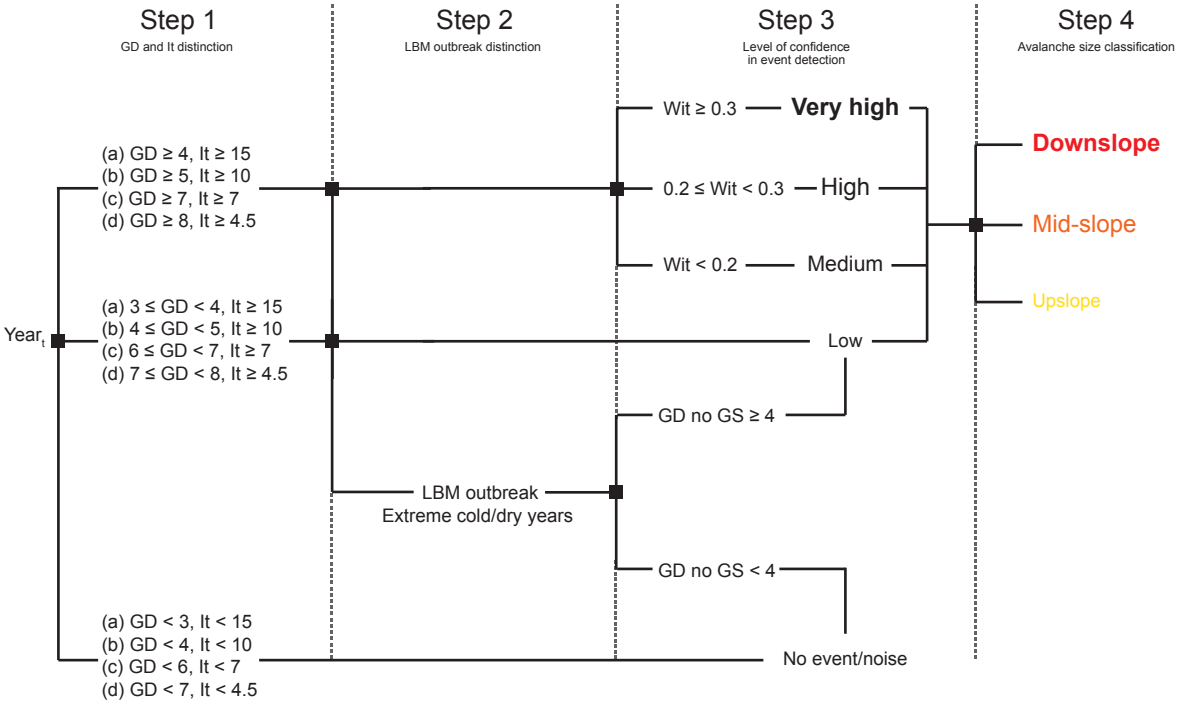
Step 1
GD and It distinction
Step 2
LBM outbreak distinction
Step 3
Level of confidence in event detection
Step 4
Avalanche size classification
Year$_t$
(a) GD ≥ 4, It ≥ 15
(b) GD ≥ 5, It ≥ 10
(c) GD ≥ 7, It ≥ 7
(d) GD ≥ 8, It ≥ 4.5
(a) 3 ≤ GD < 4, It ≥ 15
(b) 4 ≤ GD < 5, It ≥ 10
(c) 6 ≤ GD < 7, It ≥ 7
(d) 7 ≤ GD < 8, It ≥ 4.5
(a) GD < 3, It < 15
(b) GD < 4, It < 10
(c) GD < 6, It < 7
(d) GD < 7, It < 4.5
LBM outbreak
Extreme cold/dry years
Wit ≥ 0.3
Very high
0.2 ≤ Wit < 0.3
High
Wit < 0.2
Medium
Low
GD no GS ≥ 4
GD no GS < 4
No event/noise
Downslope
Mid-slope
Upslope

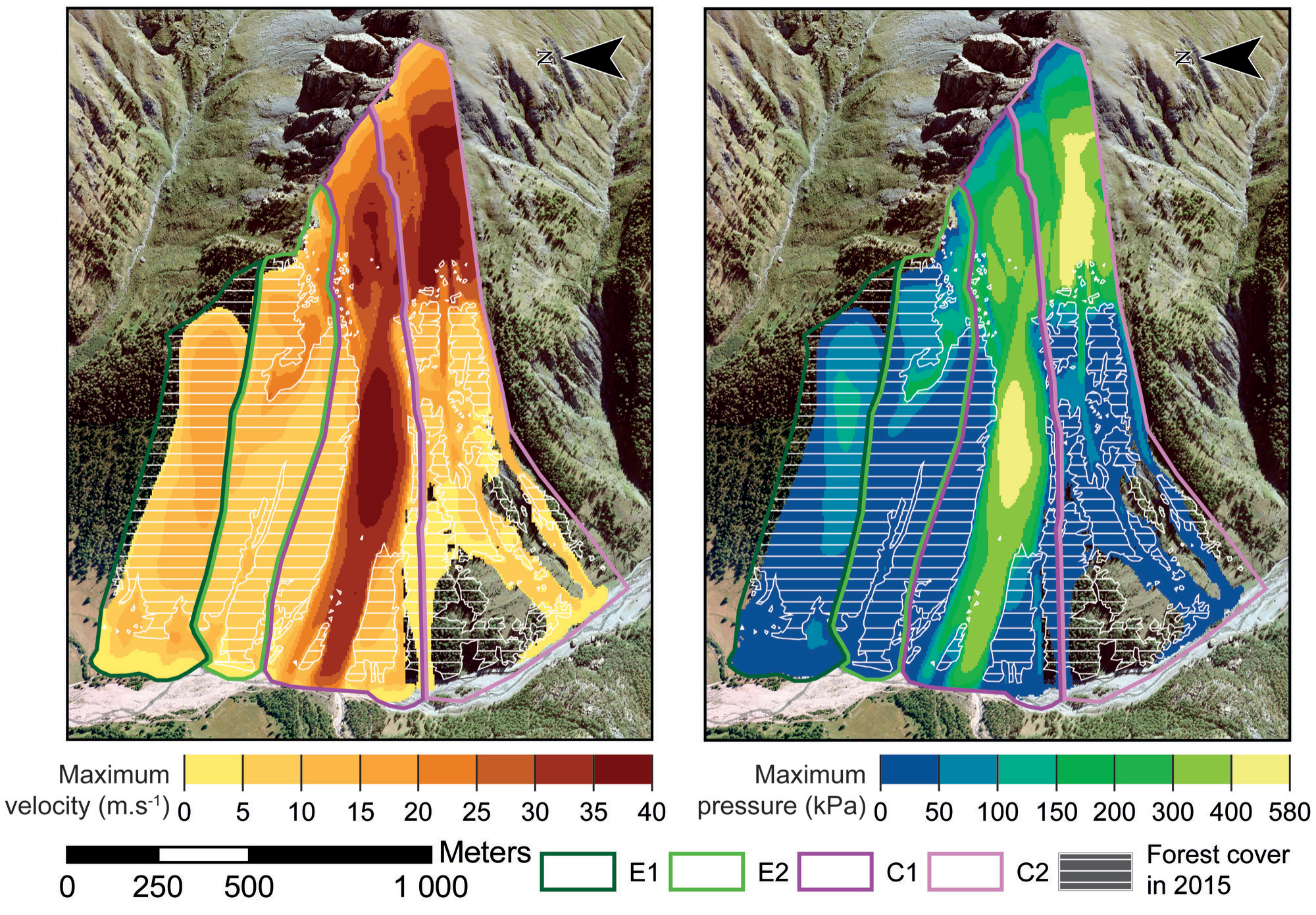
N
N
Maximum velocity (m.s-1)
0 5 10 15 20 25 30 35 40
Maximum pressure (kPa)
0 50 100 150 200 300 400 580
Meters
0 250 500 1 000
E1
E2
C1
C2
Forest cover in 2015

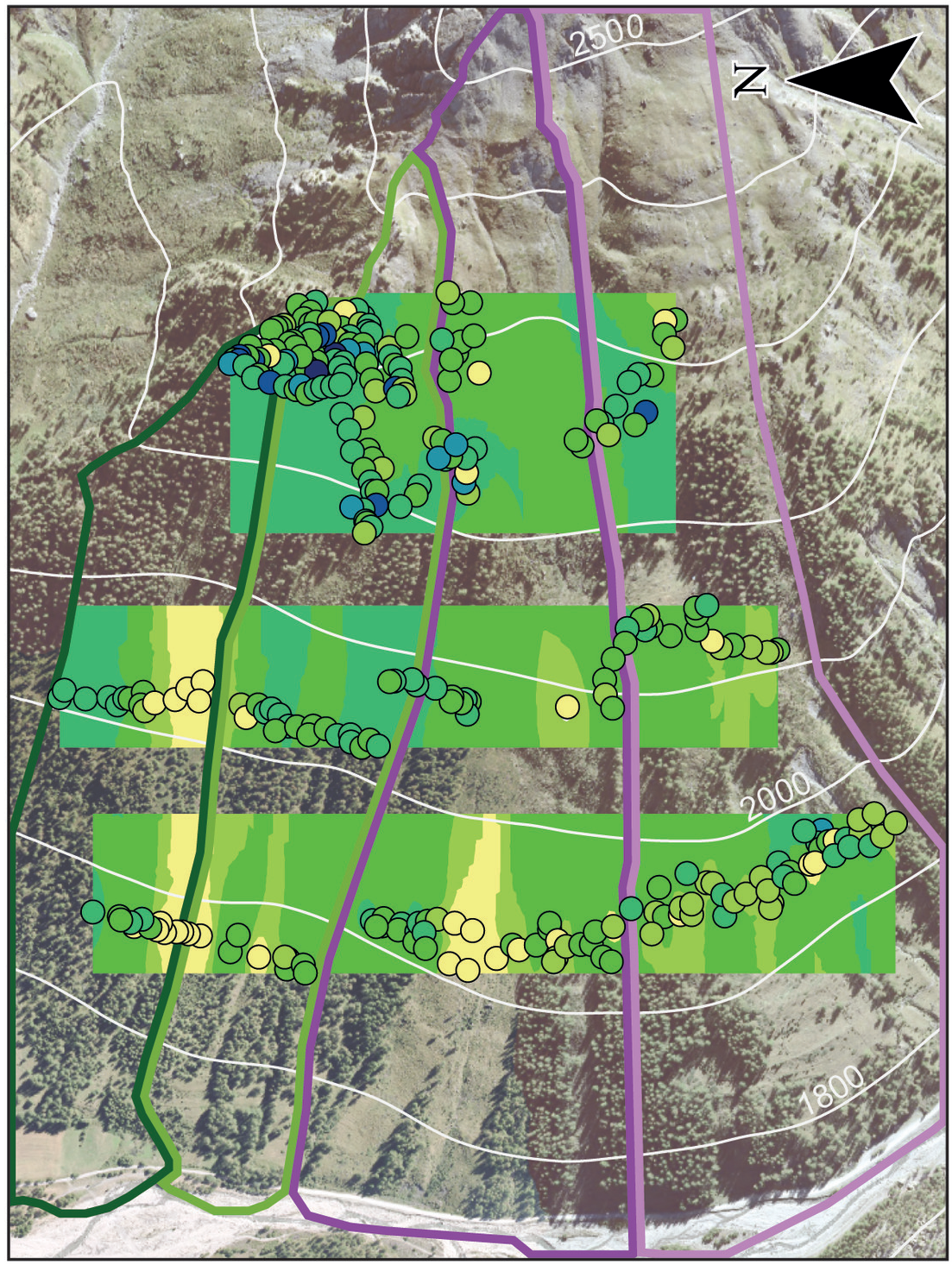

Meters

0 250 500

Tree age (yr)

Forest age structure (yr)

6 50 100 200 300 400 500 630

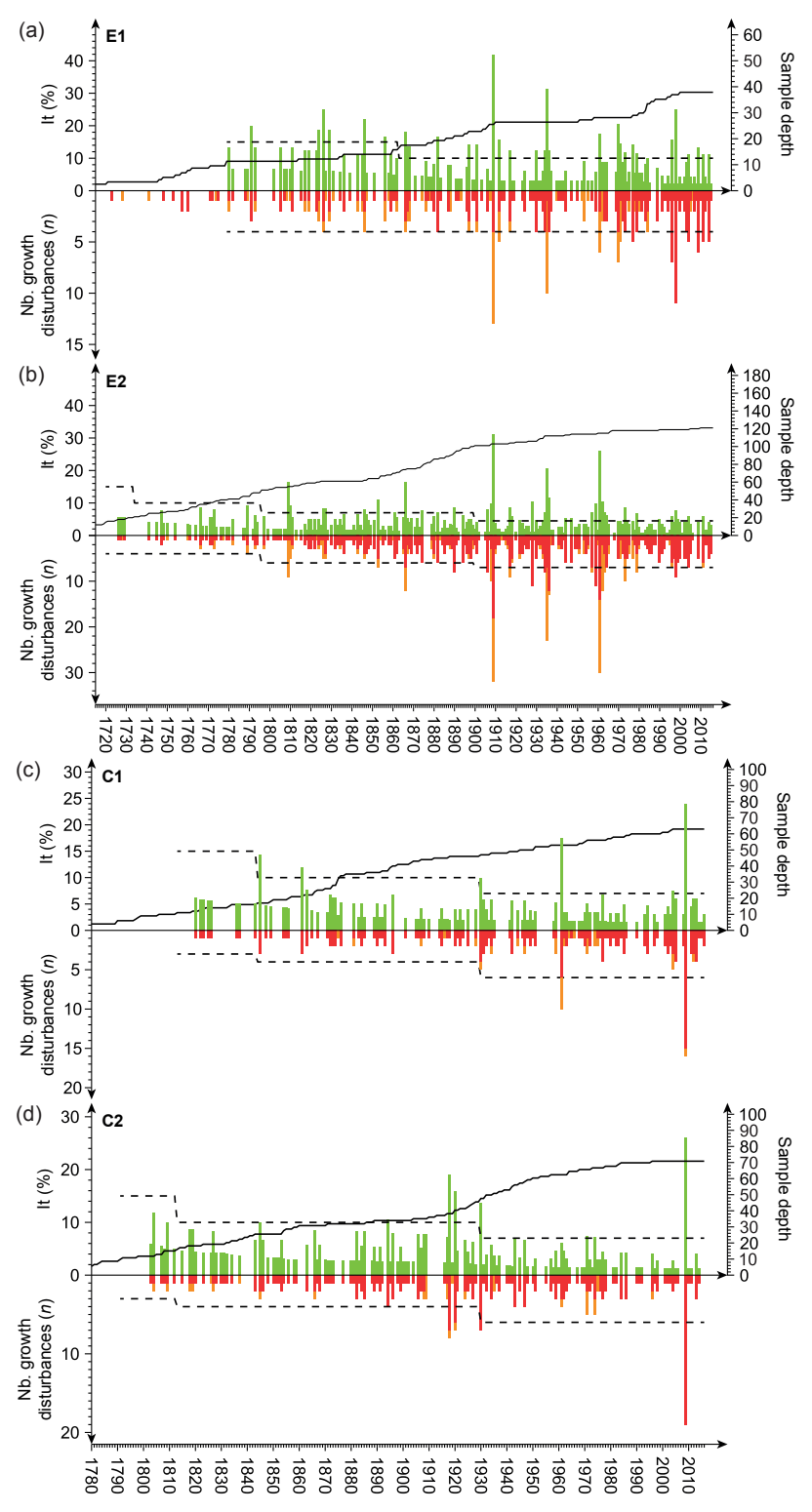
(a)
E1
It (%)
Nb. growth disturbances (n)
Sample depth
(b)
E2
It (%)
Nb. growth disturbances (n)
Sample depth
(c)
C1
It (%)
Nb. growth disturbances (n)
Sample depth
(d)
C2
It (%)
Nb. growth disturbances (n)
Sample depth

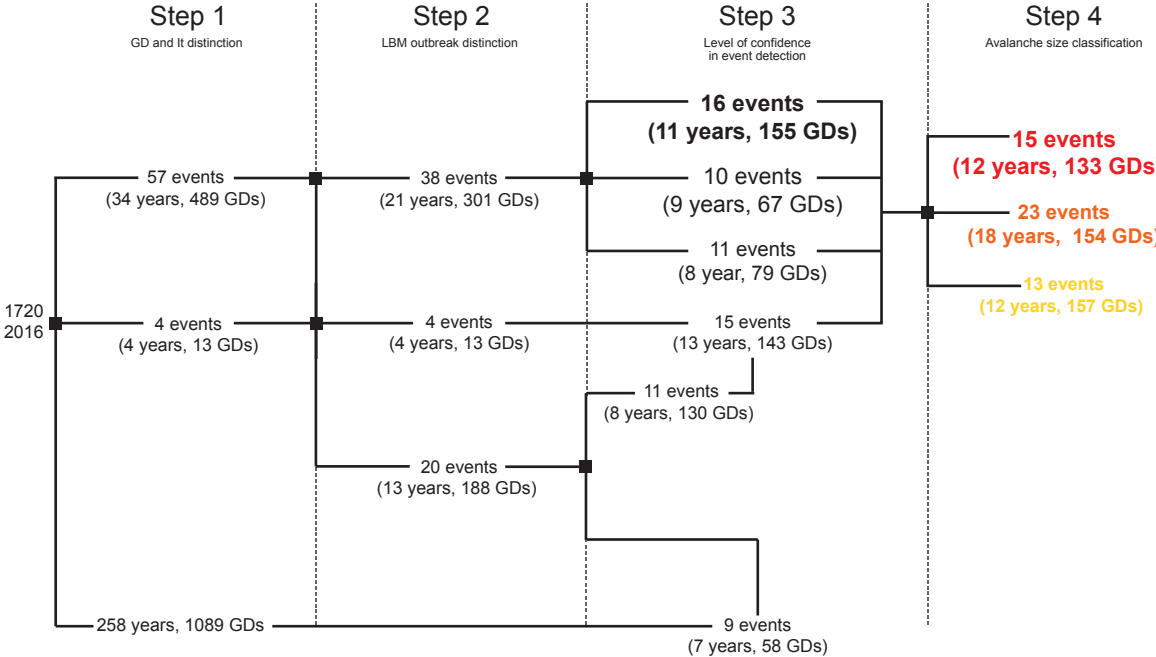
Step 1
GD and It distinction
Step 2
LBM outbreak distinction
Step 3
Level of confidence in event detection
Step 4
Avalanche size classification
1720
2016
57 events
(34 years, 489 GDs)
38 events
(21 years, 301 GDs)
16 events
(11 years, 155 GDs)
10 events
(9 years, 67 GDs)
11 events
(8 year, 79 GDs)
15 events
(12 years, 133 GDs)
23 events
(18 years, 154 GDs)
13 events
(12 years, 157 GDs)
4 events
(4 years, 13 GDs)
4 events
(4 years, 13 GDs)
15 events
(13 years, 143 GDs)
11 events
(8 years, 130 GDs)
20 events
(13 years, 188 GDs)
258 years, 1089 GDs
9 events
(7 years, 58 GDs)

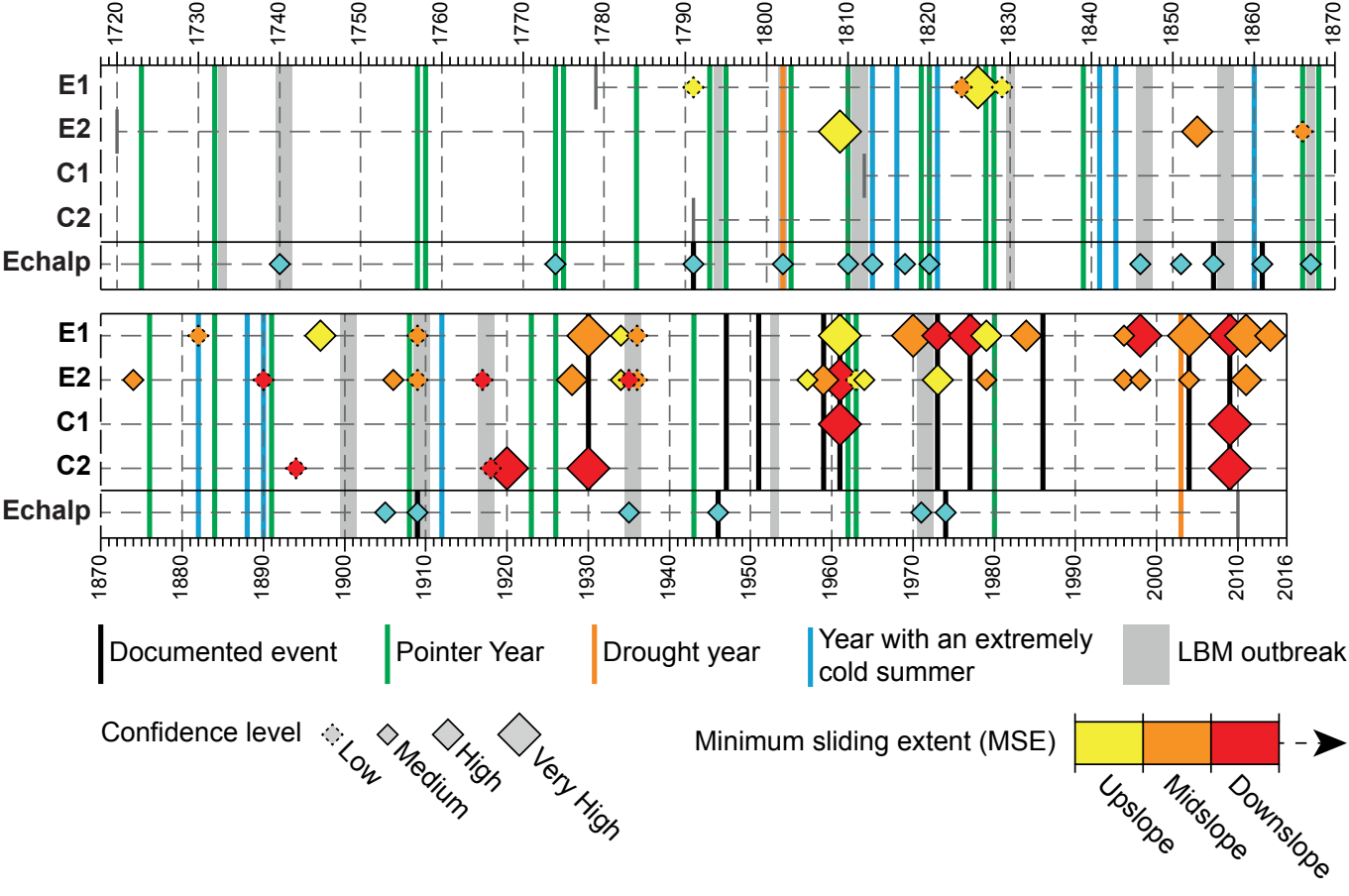
1720
1730
1740
1750
1760
1770
1780
1790
1800
1810
1820
1830
1840
1850
1860
1870
E1
E2
C1
C2
Echalp
1870
1880
1890
1900
1910
1920
1930
1940
1950
1960
1970
1980
1990
2000
2010
2016
Documented event
Pointer Year
Drought year
Year with an extremely cold summer
LBM outbreak
Confidence level
Low
Medium
High
Very High
Minimum sliding extent (MSE)
Upslope
Midslope
Downslope

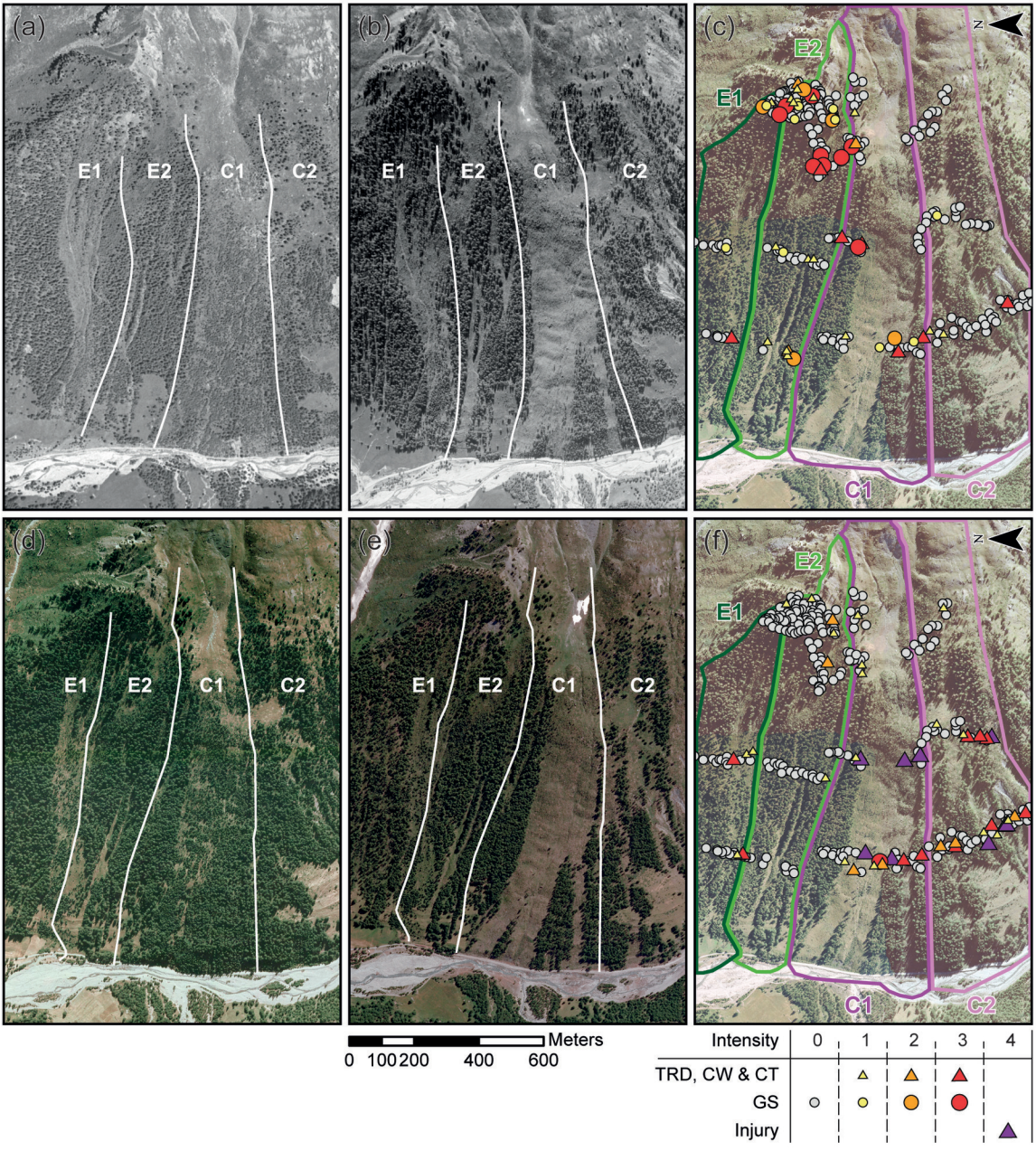
(a)
E1
E2
C1
C2
(b)
E1
E2
C1
C2
(c)
N
E2
E1
C1
C2
(d)
E1
E2
C1
C2
(e)
E1
E2
C1
C2
(f)
N
E2
E1
C1
C2
Meters
0 100200 400 600
Intensity 0 1 2 3 4
TRD, CW & CT
GS
Injury

2005**	*1884**	1818*
1980	*1883*	1815*
1971	*1876*	**1812**
1963	*1868*	**1811**
1962	**1867**	*1810*
1943	*1866*	1804**
1936	1862*	*1803*
1935	**1857**	**1802**
1926	**1856**	*1795*
1923	**1847**	**1794**
1918	**1846**	*1793*
1917	1845*	*1784*
1914*	1843*	*1775*
1911*	*1839*	*1774*
1910	*1830*	*1758*
1909	*1828*	*1757*
1908	*1827*	**1741**
1900	1823*	**1740**
1892*	*1821*	**1733**
1891	*1820*	*1732*
*1890**	*1819*	*1723*

LBM-outbreak year, *Pointer year* , *

Path	Avalanche path							Release area				
	Aspect	Length (m)	Width (m)	Area (ha)	Mean slope (°) (SD)	Release altitude (m)	Deposit altitude (m)	Mean slope (°) (SD)	Area (ha)	Forest cover in 1945 (%)	Forest cover in 2015 (%)
E1	WN	1240	240	19.7	25.1 (9.2)	2110-2200	1745	34.5 (2.4)	4.3	76.4	100
E2	WN	1290	255	25.3	27.8 (5.6)	2140-2340	1745	35.0 (2.3)	6.4	46.9	54.7
C1	WN	1580	300	42	26.4 (6.6)	2290-2520	1760	33.1 (3.3)	6.9	1.9	1.5
C2	WN	1600	366	55	26.6 (7.3)	2430-2620	1790	32.5 (3.9)	6.9	0	0
Echalp	W	1200	200	*n.p.*	32 (*n.p.*)	2100-2450	1700	36 (*n.p.*)	*n.p.*	*n.p.*	*n.p.*

n.p. not provided

Type / intensi	1	2	3	4	Total
Injuries	-	-	-	53 (3.2%)	53 (3.2%)
TRD, CT, CW	810 (51.3%)	220 (13.9%)	187 (11.4%)	-	1217 (76.6%)
GS	147 (9.4%)	97 (6.1%)	77 (4.7%)	-	321 (20.2%)
Total	957 (60.6%)	317 (20%)	264 (16.2%)	53 (3.2%)	1591 (100%)

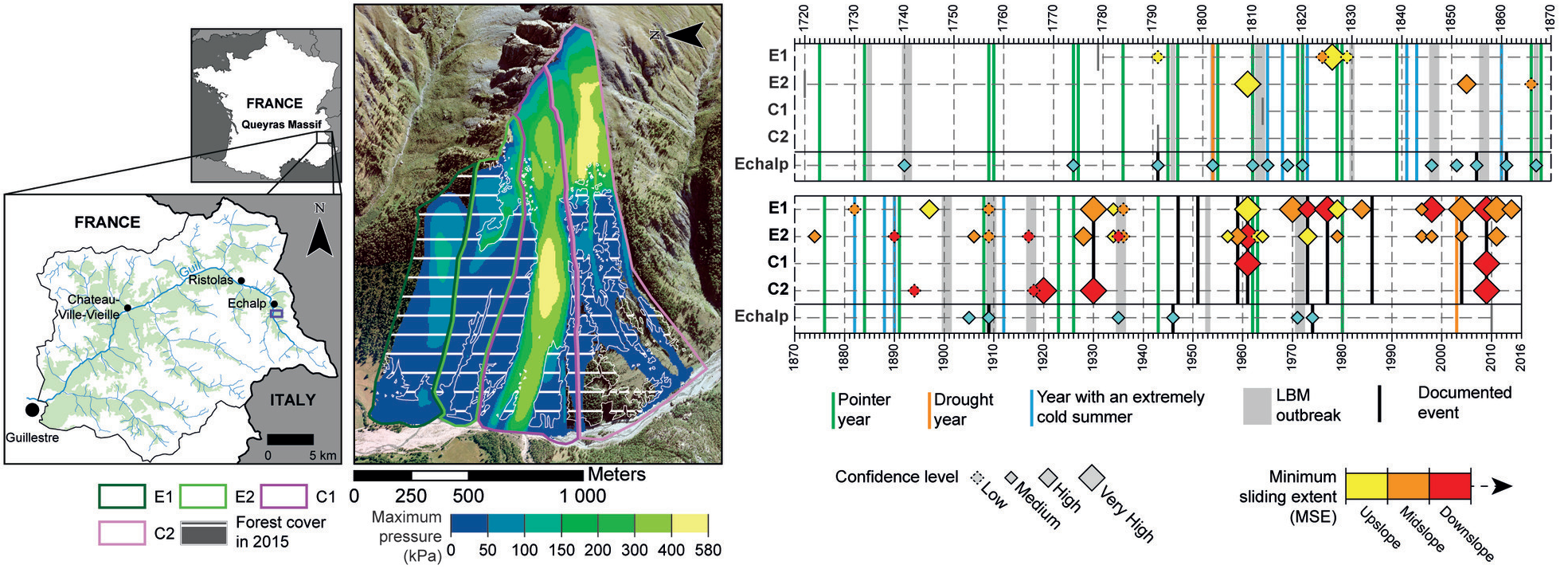
FRANCE
Queyras Massif
FRANCE
ITALY
N
Guil
Ristolas
Chateau-
Ville-Vieille
Echalp
Guillestre
0
5 km
N
Meters
0
250
500
1 000
E1
E2
C1
C2
Forest cover
in 2015
Maximum
pressure
(kPa)
0
50
100
150
200
300
400
580
1720
1730
1740
1750
1760
1770
1780
1790
1800
1810
1820
1830
1840
1850
1860
1870
E1
E2
C1
C2
Echalp
1870
1880
1890
1900
1910
1920
1930
1940
1950
1960
1970
1980
1990
2000
2010
2016
Pointer
year
Drought
year
Year with an extremely
cold summer
LBM
outbreak
Documented
event
Confidence level
Low
Medium
High
Very High
Minimum
sliding extent
(MSE)
Upslope
Midslope
Downslope